Decreased lung fibroblast growth factor 18 and elastin in human congenital diaphragmatic hernia and animal models.

Olivier Boucherat, Alexandra Benachi, Anne-Marie Barlier-Mur, Jelena Martinovic, Bernard Thébaud, Bernadette Chailley-Heu, Jacques Bourbon

▶ **To cite this version:**

Olivier Boucherat, Alexandra Benachi, Anne-Marie Barlier-Mur, Jelena Martinovic, Bernard Thébaud, et al.. Decreased lung fibroblast growth factor 18 and elastin in human congenital diaphragmatic hernia and animal models.. American Journal of Respiratory and Critical Care Medicine, 2007, 175 (10), pp.1066-77. 10.1164/rccm.200601-050OC . inserm-00130764

HAL Id: inserm-00130764

https://inserm.hal.science/inserm-00130764

Submitted on 4 Jun 2014

HAL is a multi-disciplinary open access archive for the deposit and dissemination of scientific research documents, whether they are published or not. The documents may come from teaching and research institutions in France or abroad, or from public or private research centers.

L'archive ouverte pluridisciplinaire **HAL**, est destinée au dépôt et à la diffusion de documents scientifiques de niveau recherche, publiés ou non, émanant des établissements d'enseignement et de recherche français ou étrangers, des laboratoires publics ou privés.

HAL author manuscript

Decreased Lung Fibroblast Growth Factor 18 and Elastin in Congenital Diaphragmatic Hernia and Models

Olivier Boucherat[1], Alexandra Benachi[1,2], Anne-Marie Barlier-Mur[1], Marie-Laure Franco-Montoya[1], Jelena Martinovic[3], Bernard Thébaud[4], Bernadette Chailley-Heu[1], and Jacques R. Bourbon[1]

[1] Inserm U651, Créteil, France ; Université Paris 12, Faculté de Médecine, Institut Mondor de Médecine Moléculaire, Créteil, France.

[2] Université Paris-Descartes, Faculté de Médecine ; AP-HP ; Hôpital Necker-Enfants Malades, Maternité, Paris, France.

[3] Université Paris-Descartes, Faculté de Médecine ; AP-HP ; Hôpital Necker-Enfants Malades, Service de Fœtopathologie, Paris, France.

[4] Department of Pediatrics-Division of Neonatology, University of Alberta, Edmonton, Canada.

Corresponding author and address for reprint request: Jacques Bourbon, Inserm U651, Université Paris XII, Faculté de Médecine, 8 rue du Général Sarrail, 94010 Créteil, France. Phone: 33 1 49 81 37 33; Fax: 33 1 48 98 37 33; E-mail: jacques.bourbon@creteil.inserm.fr

This work was supported by a Legs Poix Grant from the Chancellerie des Universités de Paris

Running head: FGF18 and Elastin in CDH

Descriptor number: 96

Word count: 4580

HAL author manuscript inserm-00130764, version 1

HAL author manuscript inserm-00130764, version 1

Abstract

Rationale: Lung hypoplasia in congenital diaphragmatic hernia (CDH) appears to involve impaired alveolar septation. We hypothesized that disturbed deposition of elastin and expression of FGF18, an elastogenesis stimulus, occurs in CDH.

Objectives: To document FGF18 and elastin in human CDH and ovine surgical and rat nitrofen models; to use models to evaluate the benefit of treatments.

Methods: Human CDH and control lungs were collected post-mortem. Diaphragmatic hernia was created in sheep at 85d; fetal lungs were collected at 139d (term=145d). Pregnant rats received nitrofen at 12d; fetal lungs were collected at 21d (term=22d). Some of the sheep fetuses with hernia underwent tracheal occlusion (TO); some of the nitrofen-treated pregnant rats received vitamin A. Both treatments are known to promote lung growth.

Main results: Coincidental with the onset of secondary septation, FGF18 protein increased 3-fold in control human lungs, which failed to occur in CDH. FGF18 labeling was found in interstitial cells of septa. Elastin staining demonstrated poor septation and markedly decreased elastin density in CDH lungs. Consistently, lung FGF18 transcripts were diminished 60% and 83% by CDH in sheep and rats, respectively, and elastin density and expression were also diminished. TO and vitamin A restored FGF18 and elastin expression in sheep and rats, respectively. TO restored elastin density.

Conclusions: Impaired septation in CDH is associated with decreased FGF18 expression and elastic fiber deposition. Simultaneous correction of FGF18 and elastin defects by TO and vitamin A suggests that defective elastogenesis may result, at least partly, from FGF18 deficiency.

Word count: 245

Key words: alveolarization, tracheal occlusion, nitrofen, vitamin A.

HAL author manuscript inserm-00130764, version 1

INTRODUCTION

Congenital diaphragmatic hernia (CDH) is a developmental abnormality that is associated with high mortality and morbidity because of respiratory insufficiency, due to lung hypoplasia and pulmonary hypertension (1). The incidence of CDH is about 1/3,000 live births. Despite changing concepts and methodology in treatment (2), mortality rate remains high (3, 4).

CDH lungs present fewer and smaller airspaces, reduced radial alveolar count, and thicker alveolar septa (14). Clearly, this results in part from early impairment of airway branching (6), each bronchiolar end giving rise to a limited number of saccules. Changes in key control factors involved in branching morphogenesis have been consistently reported. The sonic hedgehog system was lowered at early stages in CDH and peaked later in both humans and a rat model of CDH induced by the herbicide nitrofen (7). Fibroblast growth factor (FGF) 10 was decreased in the nitrofen model (8). The expression of FGF7, known to control alveolar epithelial cell proliferation and differentiation, was decreased in the nitrofen model (8) and in a model of surgically-induced CDH in sheep (9).

However, morphogenesis of distal lung, including alveolar septation, also seems to be impaired in CDH. This disorder appears as a common feature of hypoplastic lungs, whatever the leading cause. Thus, previous studies in human pulmonary hypoplasia of various origins, including hydrops fetalis, renal anomalies, oligohydramnios, and CDH, have established retarded acinar complexity and maturation (10, 11). Elastic fiber deposition, which is essential to build alveolar walls (16-18), was reported to be disturbed in human lung hypoplasia in association with oligohydramnios (15-17) or CDH (17), and experimentally, in drainage-induced lung hypoplasia in fetal sheep (18). Moreover, in the ovine model, alveolar hypoplasia occurred in the absence of reduction in bronchiolar generations, due to late creation of hernia (19), and discontinuous, uncondensed elastin aggregates have been described in alveolar septa (20). Decreased elastin expression with less elastin deposition and disorganized distribution, have also been reported in the nitrofen-model (21).

HAL author manuscript inserm-00130764, version 1

Compared to branching morphogenesis, less is known about mechanisms that control saccular and alveolar development. FGF18 is believed to play important role. Thus, lung-targeted FGF18 overexpression inhibited distal lung development (22), whereas FGF18-null mouse fetuses displayed smaller distal airspaces and thickened septa (23). FGF18 expression markedly increases coincidently with postnatal formation of secondary septa in the rat (24), and FGF18 enhances proliferation and elastogenesis in myofibroblasts (24), the source of septal elastin. Moreover, FGFR3 is a high-affinity receptor for FGF18 (25), and alveolarization is completely abolished in mice devoid of both FGFR3 and FGFR4 (26). Thus far, FGF18 has not been documented in the developing human lung, either in normal or pathological conditions.

The potential benefit of two treatments aiming to restore lung development in CDH, namely tracheal occlusion and vitamin A administration, have been investigated in the surgical ovine model and in the rat nitrofen-model, respectively. In sheep fetuses with hernia as well as with lung hypoplasia induced by drainage, tracheal occlusion restored lung growth, increased gas exchange surface area (27-29), and ameliorated respiratory function at delivery (30, 31). It should be emphasized that this treatment is currently under trial in human fetuses with CDH (32). In the nitrofen model, vitamin A decreased the incidence and severity of CDH, enhanced lung growth, and restored lung maturation (33, 34).

The first objective of the present study was to investigate whether CDH had impact upon FGF18 expression in the developing human lung and in models. Elastic fiber deposits and elastin expression were studied in parallel to further document qualitative and quantitative changes. The second objective consisted of using the sheep and rat models of CDH to evaluate the effects of tracheal occlusion and vitamin A-treatment, respectively, on pulmonary FGF18 expression and elastin deposition. Some of the results of these studies have been previously reported in the form of an abstract (35).

(**Word count**: 632)

HAL author manuscript inserm-00130764, version 1

MATERIAL AND METHODS

Human lung tissue

Human lung samples were collected during the autopsy after medical terminations of pregnancy in bad-prognosis fetuses, or following death after delivery. Parents were informed about the procedure and issues of post-mortem study, and signed consent was obtained for all included patients. The study received approval from the local Ethics Committee. Detailed clinical data are depicted in table 1.

Sheep model of CDH and tracheal occlusion

Surgical procedures have been extensively described elsewhere (36). Biological samples were collected from the same animals as in previous reports (20, 27).

Nitrofen exposure in rats

The procedure has been described in detail elsewhere (33). Pregnant Wistar rats were gavaged with nitrofen in olive oil on day 12. Control dams received olive oil. Vitamin A was gavaged on day 14. Fetuses were retrieved on day 21.

Histochemical elastin staining and quantification

Because of restrictions in human tissue sampling conditions, and of collection of sheep lung samples for multiple purposes (20, 27), lungs were not fixed at constant pressure. Human and sheep lungs tissue were fixed 24h after death and at sacrifice, respectively. Sections were stained for elastin with Weigert's stain. Proportion of tissue surface-area occupied by elastic fibers was determined with Perfect Image v7.4 software. In each analyzed field, tissue area was determined by subtracting airspace surface-area from total surface-area. Stained elastic fiber surface-area was measured after exclusion of large vessel and airway elastin.

HAL author manuscript inserm-00130764, version 1

Immunohistochemical FGF18 analyses

Sections were labeled using a polyclonal antibody raised in rabbit (AbCys S.A., Paris, France), and Cy3-conjugated donkey anti-rabbit IgG (Jackson ImmunoResearch, Newmarket, UK).

RNA extraction

Total RNA was extracted using Trizol reagent (Invitrogen, Cergy-Pontoise, France). Quality and integrity were confirmed after electrophoresis.

Determination of ovine partial cDNA sequence for FGF18

cDNAs were reverse-transcribed from sheep lung total RNAs, and partial amplification of partial cDNA sequence was performed using sense primer 5'-CTGCTGTGCTTCCAGGTTCA -3' (mouse/rat FGF18-specific sequence, GenBank accession numbers NM008005 and NM019199, respectively) and antisense primer: 5'-CCGTCGTGTACTTGAAGGGC -3' (human FGF18-specific sequence, GenBank accession # BC006245).

Northern blot analysis

Rat cDNA probes consisted of a 1,100-bp sequence for tropoelastin (gift from Dr. C. Rich, Philadelphia, PA) and a 904-bp sequence for FGF18 (gift from Dr. N. Itoh, Kyoto, Japan). Ovine tropoelastin cDNA probe was obtained by RT-PCR from RNA extracted from fetal sheep lung tissue, using ovine-specific oligonucleotide primers (37). Blots were exposed to X-Omat AR Kodak films, and signals were quantified by densitometry (NIH Image, Bethesda, MD).

Reverse Transcription and Real-time quantitative PCR

HAL author manuscript inserm-00130764, version 1

Real time PCR (ΔΔCt [threshold cycle] method) was carried out to determine amounts of FGF18 mRNA, FGFR3 mRNA, and internal reference 18S rRNA in ovine lungs. Primer sequences are reported in table 2. All measurements were performed in triplicate.

Western blot analysis

Membranes were exposed to goat anti-rhFGF18 antibody (R&D Systems, Lille, France) both diluted 1:500, washed in TTBS, then to horseradish peroxidase-conjugated donkey anti-goat IgG antibody (Santa Cruz Biotechnology, Santa Cruz, USA) and incubated in ECL reagent (Amersham Biosciences), before exposure to Kodak BioMax MS film. Signals were quantified by densitometry (NIH image).

Statistical analysis

Data are presented as mean ± se. Multiple group comparisons were made either by ANOVA and Fisher's PLSD, or by non-parametric Kruskall-Wallis analysis, depending on applicability as detailed in results. Two-group comparisons were made by Student's *t* test or by non-parametric Man and Whitney's U test, depending on applicability.

(Word count: 550)

RESULTS

FGF18 in human lungs with CDH

FGF18 protein was studied in human lung samples by western blot analysis. Preservation of RNA was not constant enough to perform study at pre-translational level. Because FGF18 had never been documented in developing human lung, a first step consisted in studying changes in FGF18 level during the course of intra-uterine development. FGF18 proportion increased with progressing pregnancy between 14 to 37 wk (fetal age) with a particularly marked rise around 28 wk (Figure 1A). Densitometry analysis of data corrected for variations of protein loading (Figure 1B) indicated significant positive exponential correlation with time ($r = 0.865$; $p<0.001$). The highest amount observed between 32 and 37 wk (i.e. in early alveolar

HAL author manuscript inserm-00130764, version 1

stage) reached about 20 times those observed at 14-16 wk (pseudoglandular stage) and about 10 times those at 19-21 wk (canalicular stage). Interestingly, when densitometric values were gathered into 2 groups corresponding to pre-saccular stages (≤ 26wk, n=6) and saccular-alveolar stages (age ≥ 27 wk, n=8), mean FGF18 amount increased from 165 ± 69 arbitrary units (a.U.) in the former to 782 ± 138.5 a.U. in the latter (p<0.01 by t test). Six pairs of CDH and age-matched control lungs ranging from 27 to 37 wk (saccular-alveolar stages) were then studied comparatively (Figure 2A). All CDH lungs ipsilateral to hernia displayed lower FGF18 level than their respective age-matched control, and FGF18 failed to increase in CDH samples over the period, whereas control values increased about 3 times (Figure 2B).

Elastin in human lungs with CDH

Elastin staining was performed in 5 pairs of control and CDH lungs ranging from 27 to 37 wk. In control fetuses, lung parenchyma matured homogeneously during the period, with thinning of septal walls, increased proportion of airspaces, and surge of secondary septa as illustrated in Figure 3, A and C. Airspaces displayed regular distribution. Elastin staining demonstrated bundles beneath the surface of walls, and punctate, dense deposits at the tips of growing septa that considerably increased in number with maturation (Figure 3, A' and C'). Consistent with previous reports, CDH lungs displayed thicker walls, and denser tissue (Figure 3, B and D). Elastin staining also demonstrated mostly bundles in thick septa with extreme paucity of tip deposits (Figure 3, B' and D'), which illustrates deficient secondary septation. Lung vessels strongly stained for elastin and presented no noticeable difference between CDH and control lungs. Quantitative evaluation of parenchymal elastic fiber deposits was achieved by determination of the proportion of tissue surface-area occupied by elastin patches, excluding vessel and airway elastin (Table 3). The elastic fiber density was low at 27 and 29 wk with no difference between CDH and control lungs. It was considerably higher at 31, 33 and 37 wk in controls, but failed to increase in CDH lungs that all displayed much lower value than their respective age-matched controls.

HAL author manuscript inserm-00130764, version 1

FGF18 in sheep lungs with sDH and sDH+TO

Experimental groups were: surgical diaphragmatic hernia created at 85d (sDH, n=6, term=15d), sDH + tracheal occlusion (TO, n=4), and control group (n=5), all retrieved at 139d of gestation. The expression level of FGF18 in sheep lungs was determined at pre- and post-translational levels. Since ovine FGF18 cDNA sequence had not been reported previously, a first step consisted of determining it after RT-PCR amplification. Sheep lung mRNAs were retro-transcribed and amplified using 2 oligonucleotide primers chosen in the human and mouse/rat cDNA sequences in regions proximate to 5' and 3' ends and conserved among species described thus far. This allowed amplification of a 531 bp product representing a partial sequence of ovine FGF18 corresponding to positions 49 through 579 of the 621 nucleotide coding sequences of human, mouse and rat FGF18 (Figure 4A). Its predicted amino-acid sequence shared 99% homology with human, mouse, and rat FGF18 as shown by sequence alignment (Figure 4B). The ovine cDNA sequence then served to design oligonucleotide primers for use in real-time RT-PCR, to evaluate FGF18 expression level among the various experimental groups. We found a 60% reduction of FGF18 transcript in the lung ipsilateral to hernia in the sDH group compared to control group (Figure 5A). There was a trend toward a decrease of FGF18 mRNA level in contralateral lung as well, but the difference was not statistically significant. FGF18 mRNA level was increased to twice the control level in both ipsilateral and contralateral lungs in the sDH+TO group (Figure 5A). FGF18 was also appraised at the post-translational level through western blot analysis in ipsilateral lung. FGF-18 antibody raised against the human peptide recognized ovine FGF18 at the same apparent molecular weight (Figure 5B). Densitometric analysis normalized for gel loading indicated values of 193.4 and 596.5, 23.3 and 70.1, and 1381.0 and 327.5 a.U. in controls, sDH, and sDH+TO, respectively. Consistent with mRNA findings, FGF18 protein was therefore decreased to very low level in sDH compared to controls, and re-established in sDH+TO.. Because FGFR3-FGFR4 double null mutation abolished alveolar septation in the mouse (26), and FGFR3 is a putative receptor of FGF18 (25), expression of the transcript of

HAL author manuscript inserm-00130764, version 1

FGFR3 was studied in parallel. By contrast with FGF18, FGFR3 expression was unaffected by sDH, and although it tended to increase after TO, the difference was not statistically significant (Figure 5C).

Elastin in sheep lungs with sDH and sDH+TO

Elastin staining on sections from the lung ipsilateral to hernia showed changes in elastin deposition quite similar to those in human CDH. Control lungs displayed regularly distributed airspaces with thin parenchymal tissue and dense focal elastic fiber deposits localized primary at the tips of newly forming septa and lining alveolar walls (Figure 6A, A'). All sDH lungs appeared immature with thicker septa. Some presented regularly distributed airspaces with evenly distributed elastin fibers, but similar to human CDH lungs, secondary crests with typical punctate elastin deposit at the apex were rare (Figure 6B). Other subjects displayed zones of dilated airspaces among large zones of dense and thick parenchyma, with elastin deposits being confined to dilated airspaces and extremely scarce in dense areas (Figure 6C). The paucity of elastin staining in dense areas, and its presence at the tip of septa in dilated ones indicate that the presence of dilated and non-dilated zones is not an artefactual consequence of absence of pressure fixation, but rather an actual feature of these lungs. In fetuses with sDH+TO, alveolarization appeared to be restored as indicated by reappearance of regular elastin lining and punctate elastin deposits located at the tip of crests, which presented an appearance similar to that observed in controls (Figure 6D, D'). Elastin in walls of blood vessels and airways did not appear to be altered in sDH and sDH+TO groups. Quantification of parenchymal elastic fiber density indicated dramatically reduced amounts in sDH lungs that were only one seventh those in control lungs; TO restored the proportion of elastin deposits to a level not significantly different from that in control lungs (Table 4). In addition, tropoelastin mRNA level was decreased about half in ipsilateral lung in the sDH group, but was unchanged in contralateral lung, and TO enhanced the level to twice that in controls in both ipsilateral and contralateral lungs (Figure 7), thus abolishing DH effect.

HAL author manuscript inserm-00130764, version 1

Expression of tropoelastin and FGF18 in rat lungs with induced CDH and CDH + vitA

Nitrofen treatment resulted in lung hypoplasia in all fetuses, associated with a 60 to 70% incidence of right-sided CDH. Lung wet weights were 111.1 ± 1.0, 85.5 ± 1.9, and 67.7 ± 1.6 mg in control fetuses (given olive-oil, the vehicle of nitrofen), nitrofen-treated fetuses without CDH, and nitrofen-treated fetuses with CDH, respectively (p<0.001 vs controls for both nitrofen-treated groups). Vitamin A increased lung growth without fully restoring control level in nitrofen-treated fetuses (97.8 ± 3.0 mg without CDH, and 76.0 ± 1.9 mg with CDH, p<0.05 as compared with nitrofen-treated fetuses without vitA). Tropoelastin and FGF18 mRNAs were deeply decreased to about 13% and 17% of control levels, respectively, in fetuses with nitrofen-induced CDH as compared with controls (Figure 8). Similar decreases were observed also in nitrofen-treated fetuses without CDH (not shown), suggesting association with nitrofen-induced lung hypoplasia, either in the presence or absence of hernia. Vitamin A administration 2 days after nitrofen treatment prevented the drop of both tropoelastin and FGF18 mRNAs that displayed levels not significantly different from those in controls (Figure 8).

FGF18 immunolocalization in lung tissues

This investigation was carried out in control lung tissues of the three species to define cell localization of FGF18. Figure 9 shows results obtained with the same anti-FGF18 antibody in distal lung tissue. Immunoreactivity appeared in parenchymal cells as a dotted labeling. Figure 9A depicts immunofluorescence micrograph of 37-wk fetal human lung tissue, indicating presence of FGF18 in septal cells. Epithelial airway cells were slightly labeled, whereas smooth muscle cells of small airways or arteries were negative. In bronchial cartilagenous plates, chondrocytes, which are known to express FGF18 (37), were also labeled (not shown). In 139d fetal sheep lung tissue (Figure 9C), labeling was similarly found in septa. Weak labeling was also present in airway epithelial cells (not shown), but was absent from airway and vascular smooth muscle cells. In the rat, we choose to study lung tissue on postnatal day 4 (Figure 9E), when FGF18 expression has been reported to be

HAL author manuscript inserm-00130764, version 1

elevated (24). FGF18 immunoreactivity was present in cells in the thickness of walls of primary as well as secondary septa (left and right inserts in Figure 9E, respectively). Distribution of FGF18 labeling appeared similar to that of elastin or alpha smooth muscle actin (Figure 9G).

DISCUSSION

We report that decreases of FGF18 expression and of elastic fiber deposition in alveolar septa characterize CDH in humans. The presence of similar features in two animal models allowed us to use the latter to evaluate the effects of potential therapeutic approaches on these abnormalities. Tracheal occlusion in the surgical model, and vitamin A treatment in the nitrofen model allowed nearly normal features to be recovered. The work supports further studies to determine the potential benefit of these treatments in promoting lung growth and maturation in the presence of diaphragmatic hernia.

Limitations of the study

Investigations in humans raise the question of control appropriateness. Only lung samples from subjects with other, non-pulmonary diseases, can be used as controls. This is clearly an unavoidable limitation of the present study that may introduce bias. For instance, FGF18 is known to be involved not only in lung development, but also in the formation of heart, bone, and central nervous system. Nevertheless, the fact that differences were demonstrated between CDH and control lungs, and were observed also in animal models of CDH suggests that abnormalities actually result from CDH. This underlines the usefulness of comparing human and model data.

Lung expression of FGF18 is deficient in diaphragmatic hernia

Lung hypoplasia associated with CDH is believed to result from a precocious arrest of bronchial branching (6). Development of distal lung, including saccules and alveoli, appears to be impaired also. Disturbed alveolar development appears to be a common feature of

HAL author manuscript inserm-00130764, version 1

hypoplastic lungs, including in the instance of CDH (10, 11, 15-17). Altogether, these disorders result in histological appearance of less than stated gestational age with less acinar complexity (5). Taking into account the recently demonstrated association of FGF18 with alveolarization process, we investigated whether pulmonary FGF18 expression was affected in CDH lung. FGF18 was effectively shown to play a crucial role in development of murine distal lung. Similar to features seen in mice deficient in elastin (13), fewer and larger air sacs were observed in FGF18-deficient mouse fetuses (23). Although lethality at birth prevents one from studying alveolarization in FGF18-deficient mice, the involvement of FGF18 in secondary septation is supported by FGF18 up-regulation during the process in the rat (24), by elastogenesis-stimulating activity of FGF18 in fibroblasts (24), and by the crucial role of FGFR3-FGFR4 signaling for secondary septation (26).

The expression pattern of FGF18 in the developing human lung had not been examined previously. A first step therefore consisted in studying FGF18 expression in the course of fetal lung development. A major observation of the present study was the marked increase in FGF18 protein, starting from 27-28 wk of gestation to reach elevated level at 36-37 wk. Although the precise time when secondary alveolar septation begins in humans is a matter of debate, in part because of the difficulty in defining an alveolus in microscopic sections (12), it is generally accepted that the process starts between 30 and 36 wk. Therefore, FGF18 increases in human lung coincidently with starting secondary septation. This finding, consistent with studies in rodents, reinforces the assumption of involvement of FGF18 in alveologenesis. Moreover, FGF18 localization in interstitial cells of alveolar walls, presumably myofibroblasts, at sites and time of alveolarization and elastin deposition strongly argues in favor of FGF18 involvement in the process. Previous investigation had consistently indicated that FGF18 expression was located principally in interstitial tissue of distal lung areas in the mouse (22). Furthermore, FGF18 absence from perivascular or peri-airway wall tissue where elastin is also abundant, is in favor of specific involvement for alveolarization at this stage of lung development.

In a second step, human CDH lungs were compared to age-matched controls. We

HAL author manuscript inserm-00130764, version 1

found low FGF18 protein level in CDH lungs, with failure to increase in late pregnancy. Consistently, lowered FGF18 expression was found also in the ovine sDH model and in the nitrofen model in rats. The absence of change in FGFR3 expression in sDH indicates impairment of signaling at the ligand level, not the receptor level. Secondary septation was begun in humans and advanced in sheep at stages when FGF18 was determined in CDH. Impaired expression is therefore likely to be related with impairment of this process. In the rat, in contrast, the process of secondary septation was not yet initiated at the stage when the study was performed. Nevertheless, both elastin and FGF18 transcripts were decreased in the nitrofen model, which suggests disturbance in the prenatal formation of saccular walls. In rat lung, FGF18 presents two developmental peaks, a 2-fold prenatal increase between fetal days 19 and 21, and a 7-fold increase between postnatal days 2 and 3, separated by a transient fall at the time of birth (24). Changes reported here correspond to inhibition of the first rise that may therefore be related to the building of saccular walls.

Elastic fiber density is diminished in diaphragmatic hernia

Deposition of elastin fibers is intrinsic to the process of saccular and alveolar wall formation. It has been assumed that septal elastin provides a critical morphogenetic force in alveolarization (12). Consistent with previous reports, CDH lungs retained an immature appearance, and rare location of elastin at the tip of growing crests supports deficiency in secondary septa. Similar observations in the ovine sDH model indicate that lung compression by ascended viscera precipitates these disorders. We did not examine elastin deposits histologically in rat fetuses with nitrofen-induced CDH, but a previous investigation in the same model (21) had demonstrated paucity of elastin staining in the simplified terminal airways, similar to our report herein for human and sheep lungs.

Decreased density of elastin fibers in distal parenchyma of CDH lungs is a novel finding of the present investigation. It indicates clearly that defective septation results from deficient elastin deposition. Decreased tropoelastin transcripts in the fetal sheep model indicated that impairment occurs at the pretranslational level. Reduced lung expansion

HAL author manuscript inserm-00130764, version 1

induced by lung fluid drainage has been reported to decrease tropoelastin mRNA 2.5-fold (38). Contradictory observations have been reported in the nitrofen model with either decreased (21 and present data) or increased (39) tropoelastin transcripts. The reason for the discrepancy between studies is unclear, but may be due to methodological differences (21). Moreover, reduced levels of tropoelastin transcripts in the nitrofen model were corroborated by reduction of desmosine content (indicative of cross-linked elastin) in the lung ipsilateral to hernia (21). Although no quantitative evaluation of elastin synthesis was performed in oligohydramnios, the absence of elastin deposits in alveolar septa reported at the ultrastuctural level in hypoplastic lungs with this disease (16) also suggests defective synthesis. Impaired elastogenesis in pulmonary septa therefore presents as a common feature in under-expanded hypoplastic lungs whatever the leading cause, and may therefore represent a direct consequence of insufficient lung-tissue tension. Although the present investigation does not demonstrate a causal relationship between FGF18 changes and impairment or restoration of alveolarization, developmental lung disturbances in prenatal mice lacking FGF18 (23), and the coordinated effects of FGF18 upon various proteins involved in elastogenesis by neonatal rat lung myofibroblasts (24) strongly argue in favor of such a link. The presence of FGF18 transcripts (22) and immunoreactive FGF18 (present data) in distal lung parenchyma reinforces this hypothesis.

Treatments restore FGF18 expression and elastin deposition in CDH models

FGF18 and elastin transcript and protein were restored or enhanced above control level by TO in sDH, and by vitamin A in the nitrofen model. It is well established that TO induces cell proliferation (40), a process enhanced for all cell types during alveolarization. A variety of growth factors have indeed been reported to increase in the lung in response to TO, including FGF7, TGFβ2, VEGF, IGFI and IGFII (9, 41-45). The notion that they play a crucial role in expansion-induced lung growth is strengthened by the observation that replacement of lung fluid, which contains growth factors, by saline, prevents lung growth normally observed following TO (46). Our finding of increased FGF18 mRNA and protein after TO

HAL author manuscript inserm-00130764, version 1

indicates stimulation by lung expansion, and adds FGF18 to growth factors listed above. With regard to elastin expression, our findings are in agreement with those from Joyce et al (38) showing a transient 2.5-fold increase of tropoelastin mRNA in the occluded fetal sheep lung. In this study, however, TO was performed on an intact lung, and was not combined with diaphragmatic hernia or drainage. Restoration of elastic fiber density and of lung histological aspect in sDH lungs indicates that TO not only restored overall lung growth, but also secondary septation, consistent with previous observation at the ultrastructural level (20). Data from other investigations indicate that this restoration appears sufficient to recover normal morphometric parameters, including radial alveolar count (27), gas-exchange surface area, and alveolar density (28).

The second therapeutic approach consisting to use vitamin A in the nitrofen model is based on the importance of retinoids, including vitamin A and its active metabolites, in the alveolarization process (47). Several studies support the hypothesis that abnormalities within the retinoid-signalling pathway contribute to etiology of CDH (48). Moreover, decreased plasma retinol and retinol-binding protein levels have been reported in human newborns with CDH (49). Restoration of FGF18 and tropoelastin expressions by vitamin A in the lung of nitrofen-treated rat fetuses is in keeping with our previous finding that FGF18 and tropoelastin expression were both up-regulated subsequently to vitamin A administration to normal rat neonates (24). This suggests that the beneficial effect of vitamin A for pulmonary hypoplasia (33) might have resulted, among possible changes in other growth factors, from promotion of FGF18 expression. However, it should be emphasized that in this model, lung hypoplasia and immaturity also occur in pups that do not develop CDH. Although less marked, the morphology of lungs of fetuses without hernia was reported to be similar to that of CDH lungs, including paucity of elastic fiber deposits in septa (21). In agreement with this observation, we found reduced FGF18 and tropoelastin expression in nitrofen-treated fetuses devoid of hernia. Disorders could therefore result from pulmonary toxic effect(s) of nitrofen, independently of CDH. The transcription factor TTF-1, which is essential to lung morphogenesis, was down-regulated by nitrofen in fetal rat lungs independently of the

HAL author manuscript inserm-00130764, version 1

presence of CDH (50), and also in a time- and dose-dependent manner in cultured lung epithelial H-441 cells (51). Last, nitrofen is also believed to interfere with vitamin A signaling (52, 53). Therefore, it cannot be excluded that vitamin A supplementation counteracted pulmonary effects of nitrofen, including FGF18 and elastin changes, that were not direct consequences of hernia. Considering the use of vitamin A as a possible treatment of lung abnormalities in CDH therefore requires further evaluation of its actual benefits and safety.

In conclusion, changes in FGF18 induced by CDH and treatments are novel and significant findings in the present study. Simultaneous correction of FGF18 and elastin defects by TO and vitamin A suggests that disordered alveolarization may result, at least in part, from FGF18 deficiency.

HAL author manuscript inserm-00130764, version 1

References

1. Kitagawa M, Hislop A, Boyden EA, Reid L. Lung hypoplasia in congenital diaphragmatic hernia. A quantitative study of airway, artery, and alveolar development. *Br J Surg* 1971; 58: 342-346.

2. Tibboel D, Bos AP, Hazebroek FW, Lachmann B, Molenaar JC. Changing concepts in the treatment of congenital diaphragmatic hernia. *Klin Padiatr* 1993; 205: 67-70.

3. Stege G, Fenton A, Jaffray B. Nihilism in the 1990s: the true mortality of congenital diaphragmatic hernia. *Pediatrics* 2003; 112: 532-535.

4. Moya FR, Lally KP. Evidence-based management of infants with congenital diaphragmatic hernia. *Semin Perinatol* 2005; 29:112-117.

5. George DK, Cooney TP, Chiu BK, Thurlbeck WM. Hypoplasia and immaturity of the terminal lung unit (acinus) in congenital diaphragmatic hernia. *Am Rev Respir Dis* 1987; 136: 947-950.

6. Areechon W, Reid L. Hypoplasia of lung with congenital diaphragmatic hernia. *Br Med J* 1963; 5325: 230-233.

7. Unger S, Copland I, Tibboel D, Post M. Down-regulation of sonic hedgehog expression in pulmonary hypoplasia is associated with congenital diaphragmatic hernia. *Am J Pathol* 2003; 162: 547-555.

HAL author manuscript inserm-00130764, version 1

8. Teramoto H, Yoneda A, Puri P. Gene expression of fibroblast growth factors 10 and 7 is downregulated in the lung of nitrofen-induced diaphragmatic hernia in rats. *J Pediatr Surg* 2003; 38: 1021-1024.

9. McCabe AJ, Carlino U, Holm BA, Glick PL. Upregulation of keratinocyte growth factor in the tracheal ligation lamb model of congenital diaphragmatic hernia. *J Pediatr Surg* 2001; 36: 128-132.

10. Wigglesworth JS, Desai R, Guerrini P. Fetal lung hypoplasia: biochemical and structural variations and their possible significance. *Arch Dis Child* 1981; 56: 606-615.

11. Nakamura Y, Harada K, Yamamoto I, Uemura Y, Okamoto K, Fukuda S, Hashimoto T. Human pulmonary hypoplasia. Statistical, morphological, morphometric, and biochemical study. *Arch Pathol Lab Med* 1992; 116: 635-642.

12. Burri P. Structural aspects of prenatal and postnatal development and growth of the lung. In: Mc Donald JA, editor. Lung growth and development. New York: Marcel Dekker; 1997. p. 1-35.

13. Wendel DP, Taylor DG, Albertine KH, Keating MT, Li DY. Impaired distal airway development in mice lacking elastin. *Am J Respir Cell Mol Biol* 2000; 23: 320-326.

14. Lindahl P, Karlsson L, Hellstrom M, Gebre-Medhin S, Willetts K, Heath JK, Betsholtz C. Alveogenesis failure in PDGF-A-deficient mice is coupled to lack of distal spreading of alveolar smooth muscle cell progenitors during lung development. *Development* 1997; 124: 3943-3953.

15. Wigglesworth JS, Hislop AA, Desai R. Biochemical and morphometric analyses in hypoplastic lungs. *Pediatr Pathol* 1991; 11: 537-549.

HAL author manuscript inserm-00130764, version 1

16. Haidar A, Ryder TA, Wigglesworth JS. Failure of elastin development in hypoplastic lungs associated with oligohydramnios: an electronmicroscopic study. *Histopathology* 1991; 18: 471-473.

17. Nakamura Y, Fukuda S, Hashimoto T. Pulmonary elastic fibers in normal lung development and in pathological conditions. *Pediatr Pathol* 1990; 10: 689-706.

18. Boland R, Joyce BJ, Wallace MJ, Stanton H, Fosang AJ, Pierce RA, Harding R, Hooper SB. Cortisol enhances structural maturation of the hypoplastic fetal lung in sheep. *J Physiol* 2004; 554: 505-517.

19. Kent GM, Olley PM, Creighton RE, Dobbinson T, Bryan MH, Symchych P, Zingg W, Cummings JN. Hemodynamic and pulmonary changes following surgical creation of a diaphragmatic hernia in fetal lambs. *Surgery* 1972; 72: 427-433.

20. Benachi A, Delezoide AL, Chailley-Heu B, Preece M, Bourbon JR, Ryder T. Ultrastructural evaluation of lung maturation in a sheep model of diaphragmatic hernia and tracheal occlusion. *Am J Respir Cell Mol Biol* 1999; 20: 805-812.

21. Mychaliska GB, Officer SM, Heintz CK, Starcher BC, Pierce RA. Pulmonary elastin expression is decreased in the nitrofen-induced rat model of congenital diaphragmatic hernia. *J Pediatr Surg* 2004; 39: 666-671.

22. Whitsett JA, Clark JC, Picard L, Tichelaar JW, Wert SE, Itoh N, Perl AK, Stahlman MT. Fibroblast growth factor 18 influences proximal programming during lung morphogenesis. *J Biol Chem* 2002; 277: 22743-22749.

HAL author manuscript inserm-00130764, version 1

23. Usui H, Shibayama M, Ohbayashi N, Konishi M, Takada S, Itoh N. Fgf18 is required for embryonic lung alveolar development. *Biochem Biophys Res Commun* 2004; 322: 887-892.

24. Chailley-Heu B, Boucherat O, Barlier-Mur AM, Bourbon JR. FGF-18 is upregulated in the postnatal rat lung and enhances elastogenesis in myofibroblasts. Am J Physiol Lung Cell Mol Physiol 2005; 288: L43-L51.

25. Hoshikawa M, Yonamine A, Konishi M, Itoh N. FGF-18 is a neuron-derived glial cell growth factor expressed in the rat brain during early postnatal development. *Brain Res Mol Brain Res* 2002; 105: 60-66.

26. Weinstein M, Xu X, Ohyama K, Deng CX. FGFR-3 and FGFR-4 function cooperatively to direct alveogenesis in the murine lung. *Development* 1998; 125: 3615-3623.

27. Benachi A, Chailley-Heu B, Delezoide AL, Dommergues M, Brunelle F, Dumez Y, Bourbon JR. Lung growth and maturation after tracheal occlusion in diaphragmatic *Am J Respir Crit Care Med* 1998; 157: 921-927.

28. Lipsett J, Cool JC, Runciman SI, Ford WD, Kennedy JD, Martin AJ. Effect of antenatal tracheal occlusion on lung development in the sheep model of congenital diaphragmatic hernia: a morphometric analysis of pulmonary structure and maturity. *Pediatr Pulmonol* 1998; 25: 257-269.

29. Nelson SM, Hajivassiliou CA, Haddock G, Cameron AD, Robertson L, Olver RE, Hume R. Rescue of the hypoplastic lung by prenatal cyclical strain. *Am J Respir Crit Care Med* 2005; 171: 1395-1402.

HAL author manuscript inserm-00130764, version 1

30. Bratu I, Flageole H, Laberge JM, Kovacs L, Faucher D, Piedboeuf B. Lung function in lambs with diaphragmatic hernia after reversible fetal tracheal occlusion. *J Pediatr Surg* 2004; 39: 1524-1531.

31 . Davey MG, Hooper SB, Tester ML, Johns DP, Harding R. Respiratory function in lambs after in utero treatment of lung hypoplasia by tracheal obstruction. *J Appl Physiol* 1999; 87: 2296-2304.

32. Jani J, Gratacos E, Greenough A, Piero JL, Benachi A, Harrison M, Nicolaides K, Deprest J; FETO Task Group. Percutaneous fetal endoscopic tracheal occlusion (FETO) for severe left-sided congenital diaphragmatic hernia. *Clin Obstet Gynecol* 2005 ; 48:910-922.

33. Thebaud B, Tibboel D, Rambaud C, Mercier JC, Bourbon JR, Dinh-Xuan AT, Archer SL. Vitamin A decreases the incidence and severity of nitrofen-induced congenital diaphragmatic hernia in rats. *Am J Physiol Lung Cell Mol Physiol* 1999; 277: L423-L429.

34. Thebaud B, Barlier-Mur AM, Chailley-Heu B, Henrion-Caude A, Tibboel D, Dinh-Xuan AT, Bourbon JR. Restoring effects of vitamin A on surfactant synthesis in nitrofen-induced congenital diaphragmatic hernia in rats. *Am J Respir Crit Care Med* 2001; 164: 1083-1089.

35. Boucherat O, Benachi A, Franco-Montoya M-L, Thebaud B, Chailley-Heu B, Bourbon JR. Impaired elastogenesis and FGF18 expression in congenital diaphragmatic hernia. *Proc Am Thor Soc* 2006; 3: A672.

36. Benachi A, Dommergues M, Delezoide AL, Bourbon J, Dumez Y, Brunnelle F. Tracheal obstruction in experimental diaphragmatic hernia: an endoscopic approach in the fetal lamb. *Prenat Diagn* 1997; 17: 629-634.

HAL author manuscript inserm-00130764, version 1

37. Ellsworth JL, Berry J, Bukowski T, Claus J, Feldhaus A, Holderman S, Holdren MS, Lum KD, Moore EE, Raymond F, Ren H, Shea P, Sprecher C, Storey H, Thompson DL, Waggie K, Yao L, Fernandes RJ, Eyre DR, Hughes SD. Fibroblast growth factor-18 is a trophic factor for mature chondrocytes and their progenitors. *Osteoarthritis Cartilage* 2002; 10: 308-320.

38. Joyce BJ, Wallace MJ, Pierce RA, Harding R, Hooper SB. Sustained changes in lung expansion alter tropoelastin mRNA levels and elastin content in fetal sheep lungs. *Am J Physiol Lung Cell Mol Physiol* 2003; 284: L643-L649.

39. Taira Y, Oue T, Shima H, Miyazaki E, Puri P. Increased tropoelastin and procollagen expression in the lung of nitrofen-induced diaphragmatic hernia in rats. *J Pediatr Surg* 1999; 34: 715-719.

40. Moessinger AC, Harding R, Adamson TM, Singh M, Kiu GT. Role of lung fluid volume in growth and maturation of the fetal sheep lung. *J Clin Invest* 1990; 86: 1270-1277.

41. Quinn TM, Sylvester KG, Kitano Y, Kitano Y, Liechty KW, Jarrett BP, Adzick NS, Flake AW. TGF-beta2 is increased after fetal tracheal occlusion. *J Pediatr Surg* 1999; 34: 701-704.

42. Muratore CS, Nguyen HT, Ziegler MM, Wilson JM. Stretch-induced upregulation of VEGF gene expression in murine pulmonary culture: a role for angiogenesis in lung development. *J Pediatr Surg* 2000; 35: 906-912.

43. Hara A, Chapin CJ, Ertsey R, Kitterman JA. Changes in fetal lung distension alter expression of vascular endothelial growth factor and its isoforms in developing rat lung. *Pediatr Res* 2005; 58: 30-37.

HAL author manuscript inserm-00130764, version 1

44. Frenckner B, Eklof AC, Eriksson H, Masironi B, Sahlin L. Insulin like growth factor I gene expression is increased in the fetal lung after tracheal ligation. .*J Pediatr Surg* 2005; 40: 457-463.

45. Hooper SB, Han VK, Harding R. Changes in lung expansion alter pulmonary DNA synthesis and IGF-II gene expression in fetal sheep. *Am J Physiol Lung Cell Mol Physiol* 1993; 265: L403-L409.

46. Papadakis K, Luks FI, De Paepe ME, Piasecki GJ, Wesselhoeft CW Jr. Fetal lung growth after tracheal ligation is not solely a pressure phenomenon. *J Pediatr Surg* 1997; 32: 347-351.

47. Massaro D, Massaro GD. Retinoids, alveolus formation, and alveolar deficiency: clinical implications. *Am J Respir Cell Mol Biol* 2003; 28: 271-274.

48. Greer JJ, Babiuk RP, Thebaud B. Etiology of congenital diaphragmatic hernia: the retinoid hypothesis. *Pediatr Res* 2003; 53: 726-730.

49. Major D, Cadenas M, Fournier L, Leclerc S, Lefebvre M, Cloutier R. Retinol status of newborn infants with congenital diaphragmatic hernia. *Pediatr Surg Int* 1998; 13: 547-549.

50. Losada A, Tovar JA, Xia HM, Diez-Pardo JA, Santisteban P. Down-regulation of thyroid transcription factor-1 gene expression in fetal lung hypoplasia is restored by glucocorticoids. *Endocrinology* 2000; 141:2166-2173.

51. Losada A, Xia H, Migliazza L, Diez-Pardo JA, Santisteban P, Tovar JA.. Lung hypoplasia caused by nitrofen is mediated by down-regulation of thyroid transcription factor TTF-1. *Pediatr Surg Int* 1999; 15: 188-191.

HAL author manuscript inserm-00130764, version 1

52. Chen MH, McGowan A, Ward S, Bavik C, Greer JJ. The activation of the retinoic acid response element is inhibited in an animal model of congenital diaphragmatic hernia. *Biol Neonate* 2003; 83:157-161.

53. Mey J, Babiuk RP, Clugston R, Zang W, Greer JJ. Retinal dehydrogenase-2 is inhibited by compounds that induce congenital diaphragmatic hernias in rodents. *Am J Pathol* 2003; 162:673–679.

HAL author manuscript inserm-00130764, version 1

Figure legends

Figure 1. Developmental changes of FGF18 protein in human fetal lung. Western blot analysis was performed in the lung of 14 fetuses without lung disease ranging from 14 to 37 wk of pregnancy (fetal age). (A) Western blot demonstrating an obvious increase of FGF18 in late gestation (top); Ponceau S stain as loader control (bottom). (B) Densitometric analysis (arbitrary units, a.U.) showing that FGF18 was strongly up-regulated in saccular-alveolar stages (≥27 wk) as compared with pseudoglandular-canalicular stages (≤26 wk), and correlated exponentially with time (r= 0.865, p<0.001).

Figure 2. FGF18 protein expression in CDH human lungs (ipsilateral lung). Western blot analysis was performed in the lung of 6 pairs of age-matched CDH and control fetuses. (A) Representative western blot showing FGF18 expression in 3 age-matched control and CDH lungs (top); Ponceau S stain as loader control (bottom). (B) densitometric analysis (arbitrary units, a.U.); individual values corrected for loading, and linear regression analysis. FGF18 protein was lower in CDH lungs than corresponding control value for all pairs, and failed to increase with time.

Figure 3. Weigert's stain of elastin in control and CDH human lungs. Representative pictures are presented in two fetuses aged 29 wk (A, A', control, B, B', CDH) and two fetuses aged 33 wk (C, C' control, D, D' CDH). Higher magnifications are from the same sections, but not necessarily from the same field. In controls, increase of the relative portion of airspaces and surge of secondary septa were observed with advancing gestation. Elastin, stained in black, was found at the tips of secondary crests (arrows), lining the surface (arrowheads), and in vessel walls (white arrowheads). CDH lungs ipsilateral to hernia presented thickened walls, with lack of changes between stages, but vessel labeling was unaffected. Crests and typical location of elastin at their tip were rarely observed. Bar = 200µm in A-D, and 20µm in A'-D'.

HAL author manuscript inserm-00130764, version 1

Figure 4. Determination of partial cDNA sequence of ovine FGF18. (A) Nucleotide sequence of the RT-PCR product and deduced amino acid sequence. (B) Alignment and comparison of ovine FGF18 amino acid sequence with those of human, mouse, and rat FGF18 proteins. Identical amino acyl residues are marked with asterisks. These data are accessible on line under GenBank accession # DQ336700.

Figure 5. FGF18 and FGFR3 expression in fetal sheep lung with sDH and sDH+TO. (A) Real-time PCR analysis of FGF18 mRNA (mean ± se on 5, 6 and 4 individual samples in controls, sDH, and sDH+TO, respectively); FGF18 mRNA level was markedly decreased by sDH in ipsilateral lung only, and enhanced to about twice the control level by sDH+TO in both lungs. (B) Western blot analysis; ovine lung FGF18 migrated at the same apparent molecular weight as human lung FGF18 (hum); it was decreased by sDH and re-established by TO. (C) RT followed by real-time PCR analysis of FGFR3 mRNA; no significant difference was observed among the different groups. Non-parametric Kruskal-Wallis multiple group comparison, and two-group comparisons by Mann-Whitney U test. *(a)* Significant difference with controls for $p<0.05$; *(b)* significant difference with sDH for $p<0.05$.

Figure 6. Weigert's elastin stain in fetal sheep lung. (A, A') control, (B, B', C, C') sDH, (D, D') sDH+TO. A', B', C' and D' are enlargements of the dotted boxes in A, B, C and D, respectively. In control lungs, elastin regularly lined alveolar walls (black arrowheads) and focused at the tip of secondary septa with a punctate appearance (arrows). Although with variable morphology (B, B' vs C,C'), sDH lungs ipsilateral to hernia displayed thickened walls, and altered elastin pattern. TO restored both lung parenchymal structure and elastin pattern. White arrowheads: blood vessels. Bar = 50µm.

Figure 7. Tropoelastin mRNA expression in fetal sheep lung with sDH and sDH+TO. Semi-quantitative Northern blot analysis (mean ± sem on 5, 6 and 4 individual samples in controls, sDH, and sDH+TO, respectively). Tropoelastin mRNA level was decreased about half by

HAL author manuscript inserm-00130764, version 1

sDH in ipsilateral lung only, and enhanced to twice the control level by sDH+TO in both lungs. Non-parametric Kruskal-Wallis multiple group comparison, and two-group comparisons by Mann-Whitney U test. *(a)* Significant difference with controls for $p<0.05$; *(b)* significant difference with sDH for $p<0.05$; *(c)* significant difference with sDH for $p<0.01$.

Figure 8. Tropoelastin and FGF18 mRNA expression in fetal rat lungs with nitrofen-induced CDH and CDH + vitamin A treatment (CDH+vitA). Both lungs were removed en-bloc and homogenized together for RNA extraction. Mean ± se of densitometric northern blot analysis on 6 individuals (21 day-old) in each group. Both transcripts were considerably reduced in CDH, and restored to control levels in CDH+vitA. Multiple group comparison by ANOVA and Fisher's PLSD. *(a)* Significant difference from control group for $p<0.05$; *(b)* significant difference from control group for $p<0.01$; *(c)* significant difference from CDH+vitA group for $p<0.001$.

Figure 9. Immunofluorescent labeling for FGF18 in distal lung. (A) 37-wk human fetus, (C) 139d sheep fetus, (E) postnatal day 4 rat. (B, D, F) corresponding nuclear counterstaining. Dotted labeling was detected in the cytoplasm of cells with a stellate shape (arrowheads in A and C, insert in A, left insert in E), and was present in primary (* and left insert in E) and secondary septa (arrows, ** and right insert in E). Perivascular smooth-muscle cells were negative (a : pulmonary artery). Arrows point to the same locations in parallel micrographs. Immunolabeling for alpha smooth muscle actin (αSMA) in rat lung (G) displayed similar distribution pattern as FGF18. (H) Negative control for FGF18 antibody. Bar = 10µm.

HAL author manuscript inserm-00130764, version 1

Table 1

Characteristics of control and CDH human fetuses

Number	Fetal Age (weeks)	Sex	Syndrome	Body weight (g)	Lung weight / Body weight ratio
1	14	M	Single ventricle	115	ND
2	16	F	Thanatophoric dwarfism	143	0.026
3	19	F	Micromelic dwarfism	364	0.016
4	21	M	Cardiopathy	550	0.028
5	22	F	Cardiopathy	900	0.029
6	24	F	Hydrocephaly	840	0.031
7	26	F	Tetralogy of Fallot	1020	0.024
8	27	F	Pfeiffer's syndrome	1300	0.019
9	28	M	Partial trisomy 13	1630	0.021
10	28	F	Achondroplasia	1520	0.021
11	29	M	Bourneville's disease	1620	0.029
12	31	F	Cardiopathy	1720	0.024
13	32	F	Hydrocephaly	2500	0.022
14	33	M	Schizencepahly	2600	0.023
15	33	M	Trisomy 21	2450	0.026
16	35	M	Hydrocephaly	2000	0.020
17	36	M	Cardiopathy	2540	0.014
18	37	F	Spina-bifida	3140	0.017
19	27	M	CDH, left	1440	0.007
20	29	M	CDH, left	1100	0.003
21	30	M	CDH, left	2120	0.006
22	31	F	CDH, left	1900	0.004
23	32	F	CDH, left	1960	0.006
24	33	M	CDH, left	3300	0.002
25	37	F	CDH, right	3350	0.005

Lung specimens were obtained from medical terminations of pregnancy except for subjects #23 and #25 who were born alive and died immediately after birth without possible resuscitation. Lungs from fetuses with non-pulmonary diseases (#1 to 18) were used as controls. Fetal age is given as post-conceptional weeks. ND: not determined

HAL author manuscript inserm-00130764, version 1

Table 2

Sequences of oligonucleotide primers used for real-time PCR

Transcript	Forward (5'-3')	Reverse (5'-3')	Expected Size (bp)
FGF18	TGAACCGGAAAGGCAAGCT	TGACATCAGGGCTGTGTAGTTGT	100
FGFR3	GACGGCACGCCCTACGT	CGTCCTCAAAGGTGACATTGC	99
18S	AAGTCCCTGCCCTTTGTACACA	GATCCGAGGGCCTCACTAAAC	70

Table 3

Density of elastic fiber deposits in lung parenchyma of age-matched control and CDH human lungs

Stage	27 wk	29 wk	31 wk	33 wk	37 wk
Elastin/Tissue (%) Control lungs	0.43 ± 0.05	0.54 ± 0.05	1.80 ± 0.22	0.79 ± 0.07	1.55 ±0.26
Elastin/Tissue (%) CDH lungs	0.44 ± 0.07	0.60 ± 0.07	0.54 ± 0.16	0.03 ± 0.02	0.33 ± 0.10
CDH/Control ratio	1.02	1.11	0.30	0.04	0.21

The proportion of total lung tissue surface-area represented by elastic fiber deposits was determined on tissue sections after Weigert's stain, using image analysis and excluding vessel and airway elastin. Each value represents the average ratio ± se of 8 to 10 determinations in fields taken at random for one individual lung (magnification x400).

HAL author manuscript inserm-00130764, version 1

Table 4

Density of elastic fiber deposits in lung parenchyma of control, sDH, and sDH+TO sheep fetuses

Groups	Controls (4)	sDH (4)	sDH+TO (4)
Elastin/Tissue (%)	8.21 ± 1.92	1. 2 ± 0.16 *	11.67 ± 3.23 ¶

The percentage of lung tissue surface-area represented by elastic fiber deposits was determined on tissue sections after Weigert's stain, using image analysis and excluding vessel and airway elastin. Each value is the mean ± se of data from 4 fetuses in each experimental group; the value in each individual lung was calculated as the average ratio of 5 determinations in fields taken at random (magnification x200). Statistical comparison by non-parametric Mann Whitney U test: * $p<0.05$ as compared with control group; ¶ $p<0.05$ as compared with sDH group; difference between sDH ±TO and control groups is not significant.

HAL author manuscript inserm-00130764, version 1

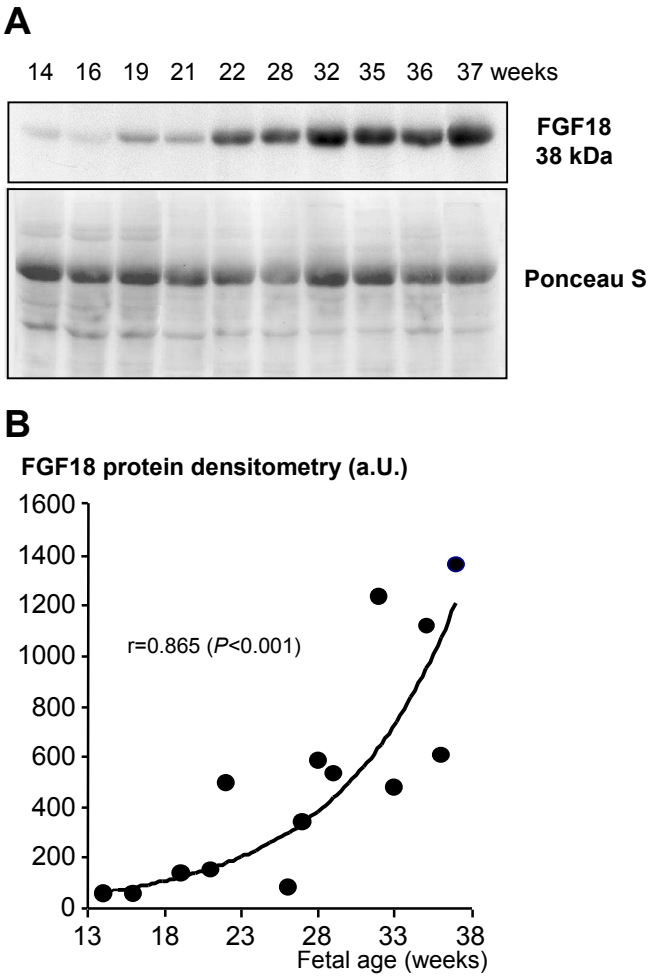

Figure 1

HAL author manuscript inserm-00130764, version 1

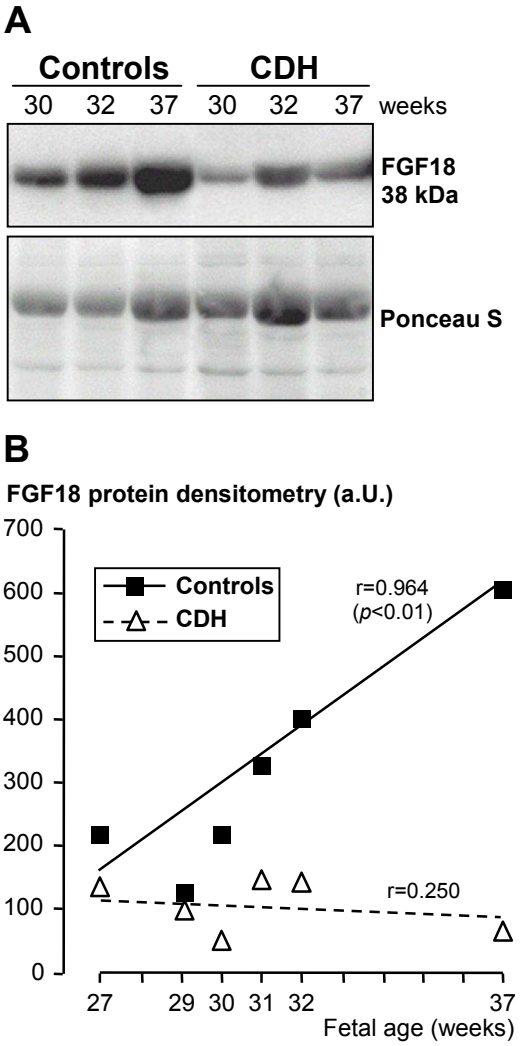

Figure 2

HAL author manuscript inserm-00130764, version 1

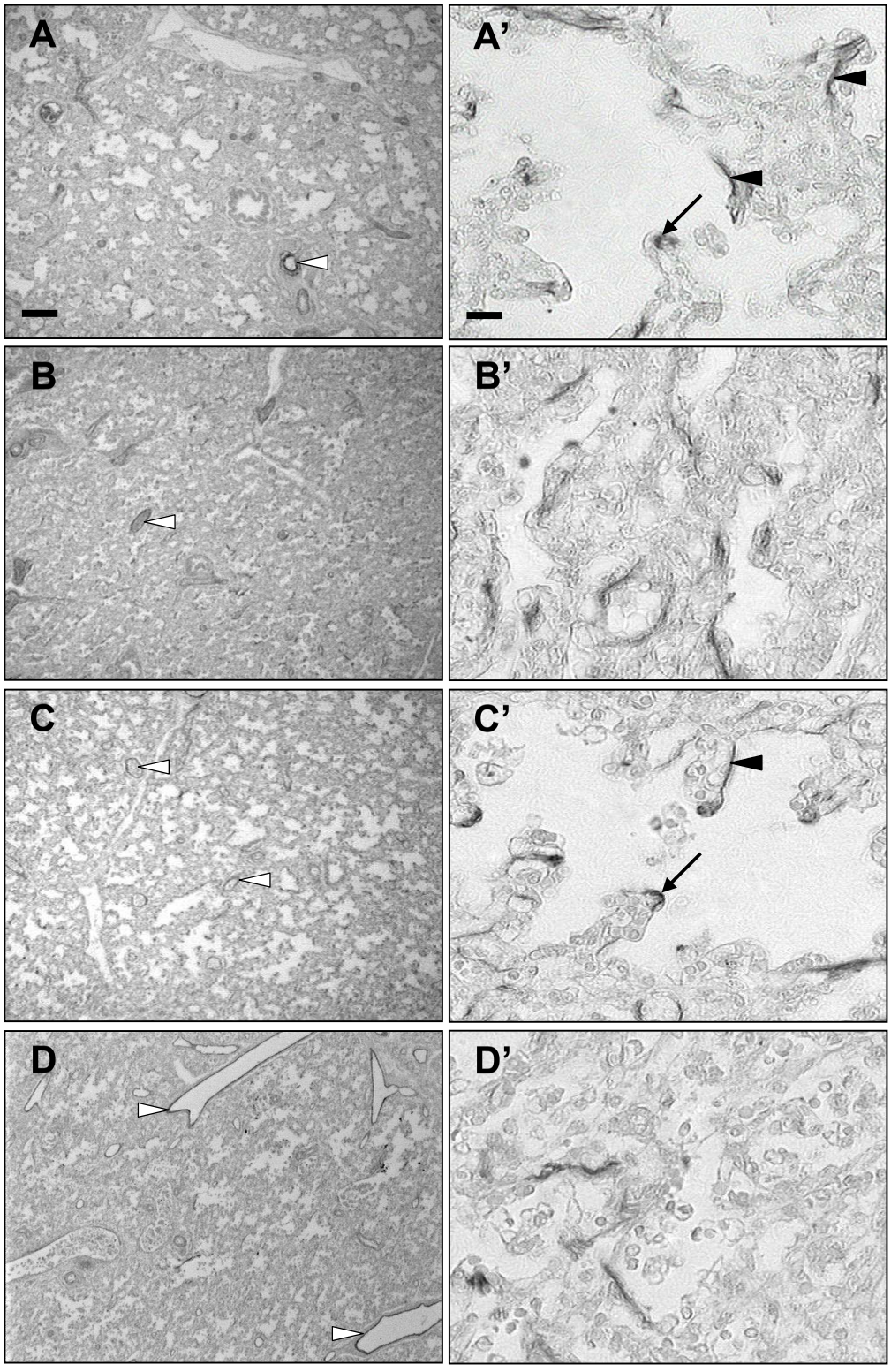

Figure 3

HAL author manuscript inserm-00130764, version 1

A

```
ctg ctg tgc ttc cag gtt cag gtg ctg gtg gcc gag gag aac gtg gac ttc cgc atc cac     60
L   L   C   F   Q   V   Q   V   L   V   A   E   E   N   V   D   F   R   I   H

gtg gag aac cag acg cgg gct cgg gac gat gtg agc cgt aag cag ctg cgg ctg tac cag   120
V   E   N   Q   T   R   A   R   D   D   V   S   R   K   Q   L   R   L   Y   Q

ctc tac agc cgg acc agc ggg aag cac atc cag gtc ctg ggc cgc agg atc agc gcc cgc   180
L   Y   S   R   T   S   G   K   H   I   Q   V   L   G   R   R   I   S   A   R

ggc gag gac ggg gac aag tat gcc cag ctc cta gtg gag aca gat acc ttc ggt agt caa   240
G   E   D   G   D   K   Y   A   Q   L   L   V   E   T   D   T   F   G   S   Q

gtc cgg atc aag ggc aag gag acg gag ttc tac ttg tgt atg aac cgg aaa ggc aag ctt   300
V   R   I   K   G   K   E   T   E   F   Y   L   C   M   N   R   K   G   K   L

gtg ggg aag cct gat ggc acc agc aaa gag tgt gtg ttc att gag aag gtt ctg gag aac   360
V   G   K   P   D   G   T   S   K   E   C   V   F   I   E   K   V   L   E   N

aac tac aca gcc ctg atg tca gct aag tac tcc ggc tgg tac gtg ggc ttc acc aag aag   420
N   Y   T   A   L   M   S   A   K   Y   S   G   W   Y   V   G   F   T   K   K

ggg cgg cca cgg aag ggc ccc aag acc cgc gag aac cag cag gat gtg cac ttc atg aag   480
G   R   P   R   K   G   P   K   T   R   E   N   Q   Q   D   V   H   F   M   K

cgc tac ccc aag gga cag gcc gaa ctg cag aag ccc ttc aag tac acg acg 3'             531
R   Y   P   K   G   Q   A   E   L   Q   K   P   F   K   Y   T   T
```

B

```
Ovine   ----------------LLCFQVQVLVAEENVDFRIHVENQTRARDDVSRKQLRLYQLYSR   60
Human   MYSAPSACTCLCLHFL*********************************************
Mouse   MYSAPSACTCLCLHFL*********A*********************************
Rat     MYSAPSACTCLCLHFL*********A*********************************

Ovine   TSGKHIQVLGRRISARGEDGDKYAQLLVETDTFGSQVRIKGKETEFYLCMNRKGKLVGKP  120
Human   ************************************************************
Mouse   ************************************************************
Rat     ************************************************************

Ovine   DGTSKECVFIEKVLENNYTALMSAKYSGWYVGFTKKGRPRKGPKTRENQQDVHFMKRYPK  180
Human   ************************************************************
Mouse   ************************************************************
Rat     ************************************************************

Ovine   GQAELQKPFKYTT-------------- 207
Human   **P**********VTKRSRRIRPTHPA
Mouse   ************VTKRSRRIRPTHPG
Rat     **T**********VTKRSRRIRPTHPG
```

Figure 4

HAL author manuscript inserm-00130764, version 1

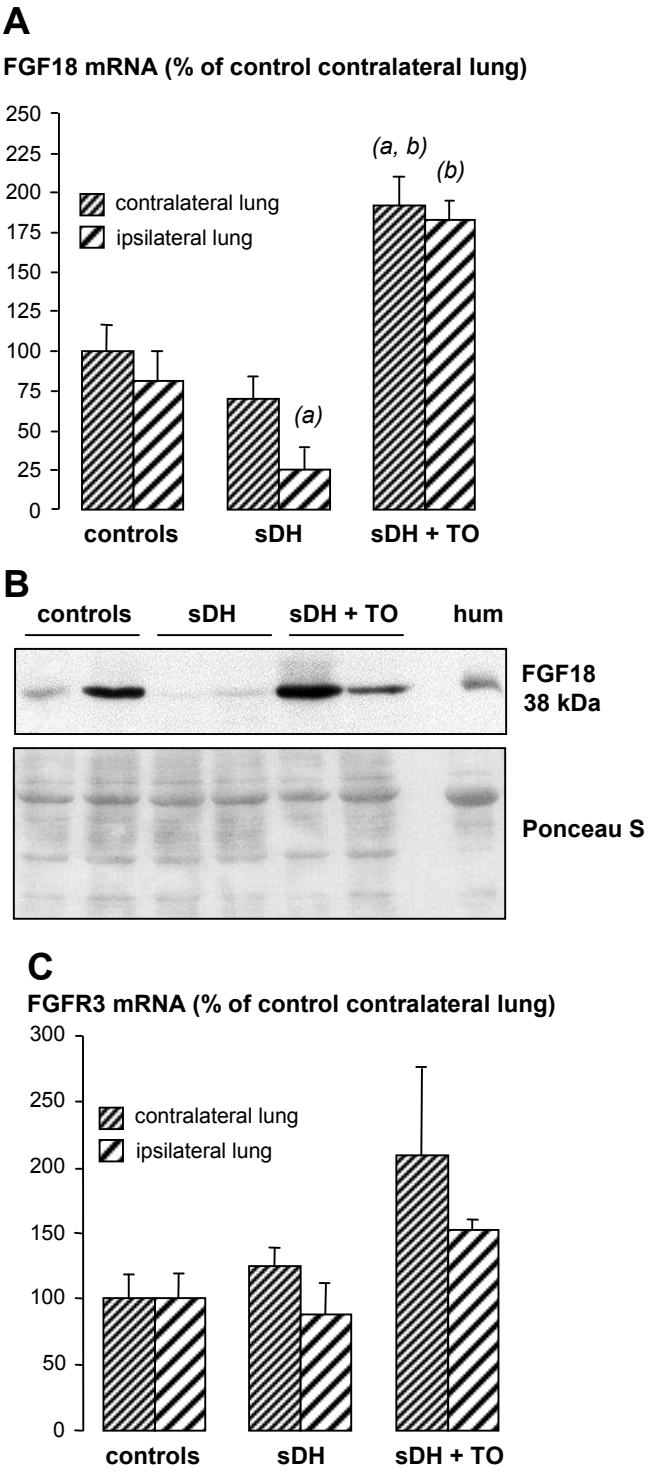

Figure 5

HAL author manuscript inserm-00130764, version 1

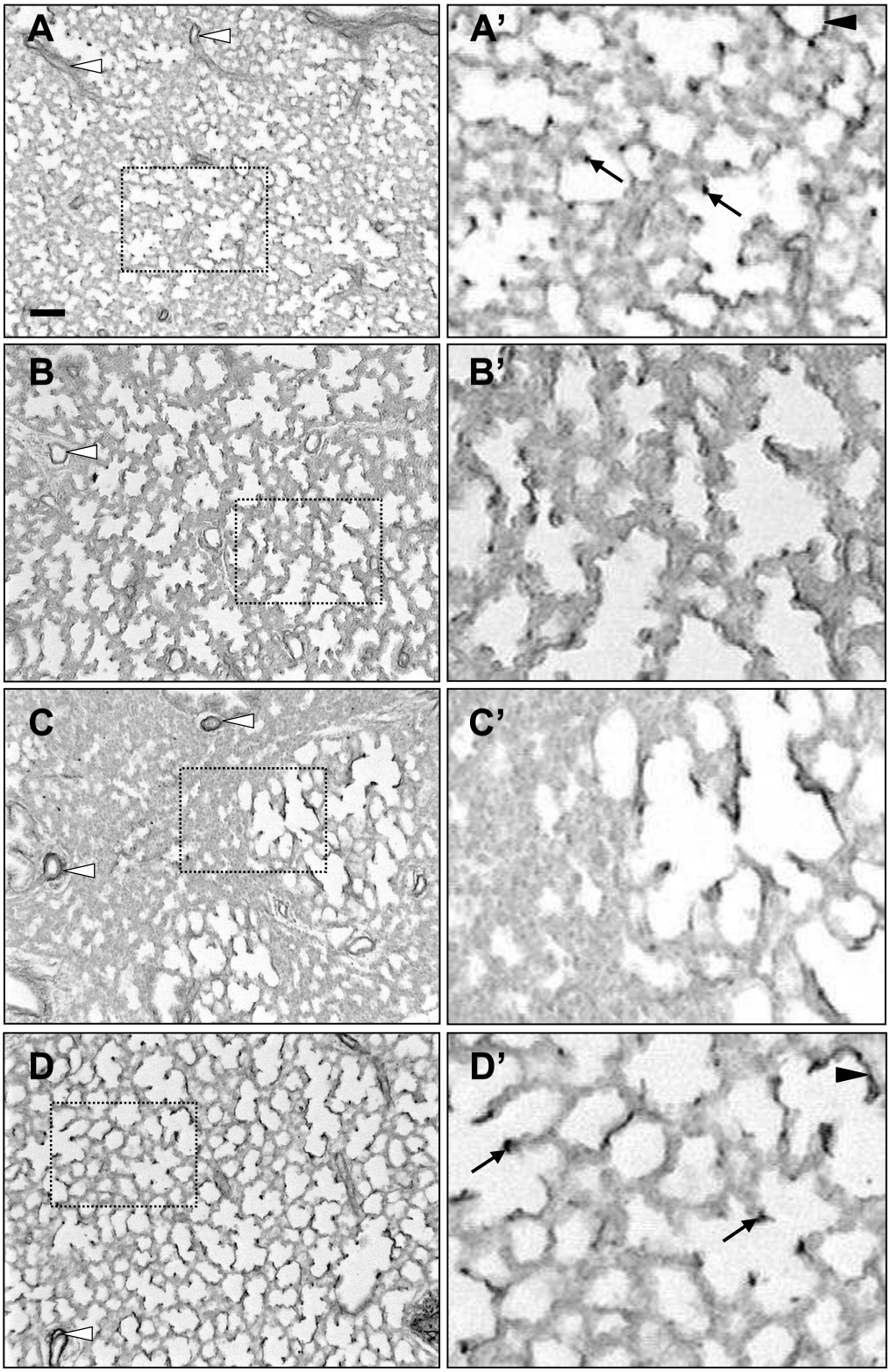

Figure 6

HAL author manuscript inserm-00130764, version 1

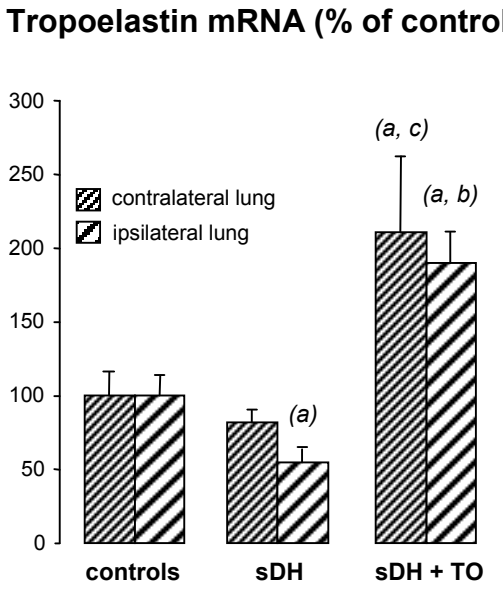

Figure 7

HAL author manuscript inserm-00130764, version 1

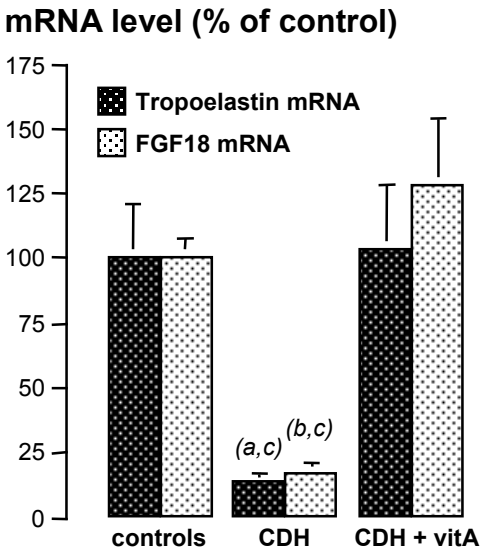

Figure 8

HAL author manuscript inserm-00130764, version 1

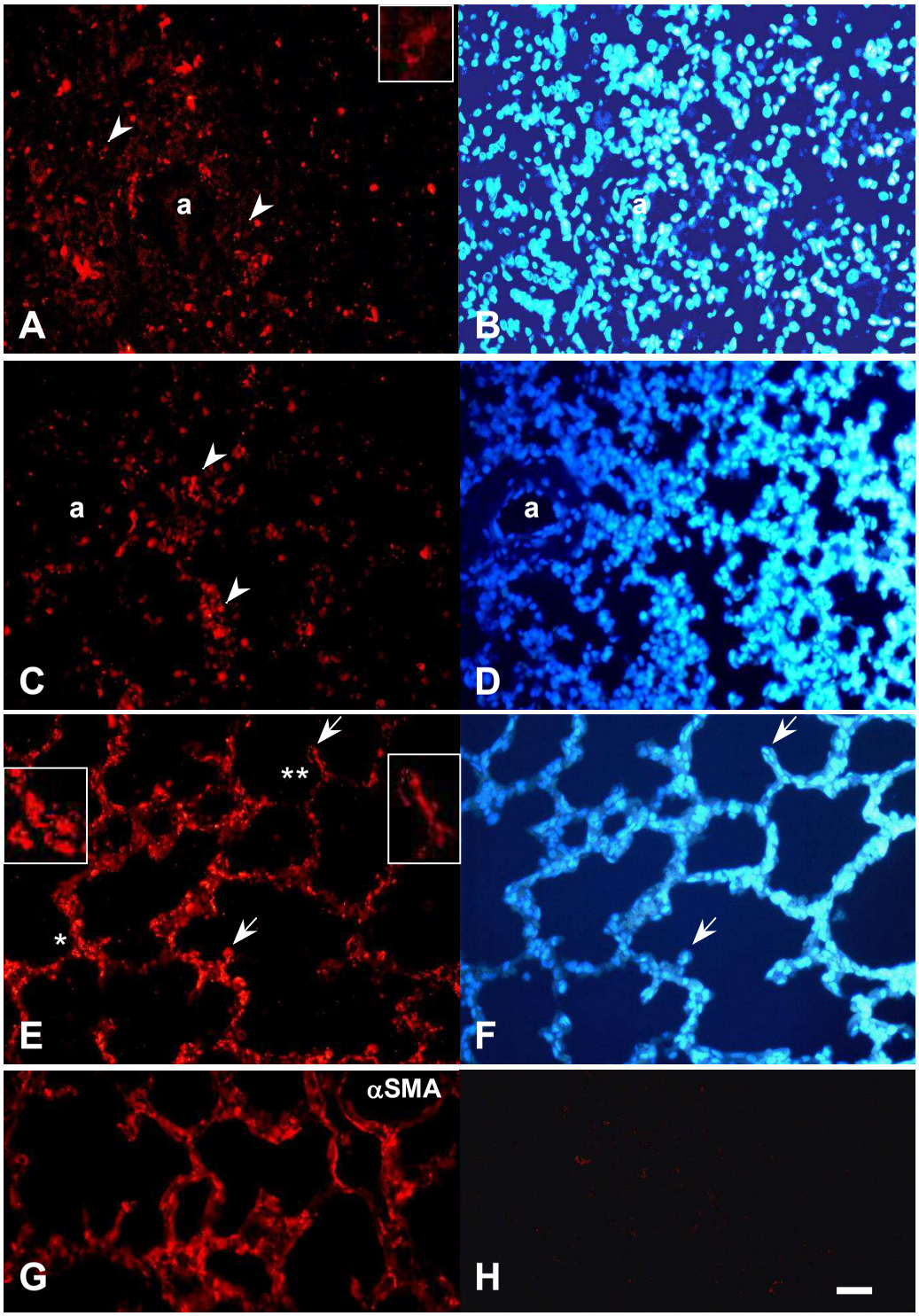

Figure 9